IOPscience iopscience.iop.org

Home Search Collections Journals About Contact us My IOPscience

Accelerated Degradation of High Power Light-Emitting Diode Resulted from Inhomogeneous Current Distribution

This content has been downloaded from IOPscience. Please scroll down to see the full text.

2011 Jpn. J. Appl. Phys. 50 034301

(http://iopscience.iop.org/1347-4065/50/3R/034301)

View the table of contents for this issue, or go to the journal homepage for more

Download details:

IP Address: 140.113.38.11
This content was downloaded on 25/04/2014 at 00:47

Please note that terms and conditions apply.

Japanese Journal of Applied Physics **50** (2011) 034301 **REGULAR PAPER**
DOI: 10.1143/JJAP.50.034301

Accelerated Degradation of High Power Light-Emitting Diode Resulted from Inhomogeneous Current Distribution

Shih Chun Yang, Pang Lin, Han Kuei Fu[1]*, An Tse Lee[1], Tzung Te Chen[1], Chien Ping Wang[1], Sheng Bang Huang[1], and Pei Ting Chou[1]

Department of Materials Science and Engineering, National Chiao-Tung University, Hsinchu 30010, Taiwan
[1]*Electronics and Optoelectronics Research Laboratories, ITRI, Chutung, Hsinchu 31040, Taiwan*

Received June 15, 2010; accepted December 22, 2010; published online March 22, 2011

The uniformity of current spreading is one of the key points to inspect the reliability and endurance of InGaN-based light-emitting diodes. In this paper, we propose an effective circuit model to analyze the phenomenon of premature turn-on diodes in the active layer. With the aging tests and novel investigation of failure analyses, the simulating results are good agreement with experimental data. It is found that an inhomogeneous distribution of forward current in light-emitting diode chips, as measured by conductive atomic force microscopes, provides the evidence that V-shaped defects and the associated threading dislocations are electrically active. Furthermore, the results of emission microscopy images and transmission electron microscope reviews support the assumption that the threading dislocations associated with V-shaped defects behave as very small shunt resistors connected across p–n junction. This study provides a degradation mechanism to realized one of the failure modes of high power light-emitting diodes. © 2011 The Japan Society of Applied Physics

1. Introduction

In recent years, high brightness light-emitting diodes (LEDs) have been successfully commercialized applied widely in many fields.[1–3] Many different degradation modes have been observed during aging. Failure mechanisms in high brightness InGaN-based LEDs also have been extensively examined for their influence on device lifetime and reliability. Actually, many processes have been found to be responsible for the degradation of InGaN-based LEDs, including as follows: (1) the generation of non-radiative defects to limit the internal quantum efficiency (IQE),[4,5] (2) the degradation of ohmic contact due to the increased material resistivity,[6] and (3) the generation of complexes involving hydrogen and the acceptor.[7]

However, a general interpretation of the physical processes under the degradation does not be investigated distinctly, due to varied stress parameters (current and temperature) and structure properties (defects, doping, and unwittingly impurities) that could lead to the different failure mechanisms. During the actual long-term operation, the major aging stresses include the injected current (electron and hole) and the heat due to joule heating by applied current, ambient, and emitting light. In this study, we are concerned with the major factor to accelerate the formation of degradation processes under the same aging condition. Therefore, six different aging conditions with the specific currents and temperatures were applied to further investigate the acceleration factors of the failure mechanisms.

2. Experiment

The available commercial 1 W blue high power light-emitting diode (HPLED) chips in this study were growth on the substrate of (0001) sapphire with standard size of $1 \times 1\,\text{mm}^2$. Figure 1 illustrates a schematic diagram of a InGaN-based LED with multiple quantum wells (MQWs) and the two-dimentional electrical model in this investigation. The overall structure consisted of a thick GaN buffer layer by low-temperature growth, an undoped GaN layer, a n-type GaN layer with the high conductivity, InGaN/GaN

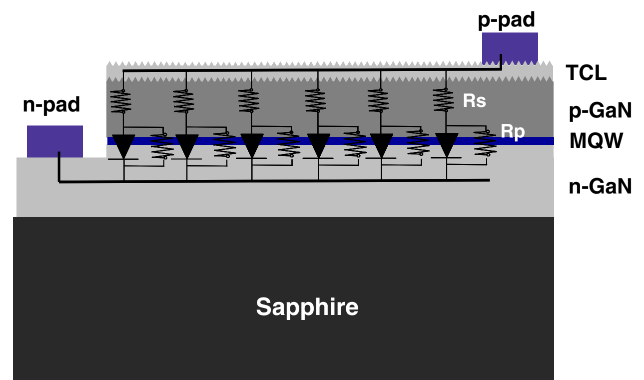

Fig. 1. (Color online) Schematic configuration of InGaN-based LED structure and two-dimensional circuit model.

MQWs active layer, and a p-type GaN layer. A thin layer of the transparent contact layer (TCL) around 300 nm thicknesses was deposited on the p-GaN layer and silicon dioxide film was deposited by the mesa to protect the sidewall of the LED device. The influence of the polymer lens in the degradation and yellowing would be non-negligible during the long-term aging. Thus, LED chips were soldered on TO-46 metallic package and sealed by the glass cap with the standard heatsink. At first, the luminous flux and the current–voltage (I–V) characteristics were collected before the aging stresses. Sixty LED devices were used under six aging conditions: 1 A/85 °C, 1 A/55 °C, 0.7 A/85 °C, 0.7 A/55 °C, 0.7 A/25 °C, and 0.35 A/25 °C. The treated devices were placed in the well-control ovens to maintain the individual specific temperatures. The currents of 350, 700, and 1000 mA were applied to a $1 \times 1\,\text{mm}^2$ chip, which currents exceeded the recommended operation current of 350 mA, and produced current densities of 35, 70, and 100 A/cm^2, respectively. Over 6000 hours of aging tests were executed to identify the long-term degradation mechanism. The emission microscopy (EMMI) was real-time used to detect accurately the sites and number of failures during the aging tests. After the long-term aging tests, both of the luminous flux and I–V characteristics were examined to select specific

*E-mail address: hkfu@itri.org.tw

 © 2011 The Japan Society of Applied Physics

aging chips to execute further examinations for investigating the degradation mechanisms of LED chips.

The following techniques are applied to observe the degeneration phenomena of LED chips and investigate the failure characterization during the long-term aging. The luminous flux was measured by the spectrometer of Instrument Systems (IS) CAS/140B and the electroluminescent (EL) mapping images were taken by ProMetric Color Model 14011 of Radiant Imaging. with Olympus BH2-UMA optical microscope. I–V characteristics were examined by Keithley 2430 sourcemeter and the localized electrical characteristics were measured through Veeco INNOVA conductive atomic force microscopes (C-AFM). In specifically destructive failure analysis, the infrared detection tool (EMMI) of Hamamatsu PHEMOS-1000 could localize the leakage path precisely and rapidly. Then, the abnormal micro-slices samples were prepared by focus ion beam (FIB) of FEI Nova-600 and the precise cross-section images were reviewed by the transmission electron microscope (TEM) of FET Tecnai Model G2F-20.

3. Results and Discussion

Figure 2(a) illustrates relative luminous flux as a function of the aging time submitted to various aging stresses. After each aging stress, the luminous fluxes were measured under the commercial driving condition of 0.35 A/25 °C and normalized to the initial value of the original devices. The luminous fluxes of all aging stresses kept decreasing in the subsequent aging process. The decrease in the luminous flux could be expressed by

$$P(t) = P(0)\exp\left(-\frac{t}{\tau}\right), \qquad (1)$$

where $P(0)$ and $P(t)$ are initial luminous flux and luminous flux after t hours, respectively.[8] The time constant of luminous degradation, τ, indicates the decrease rate of the luminous flux with aging time. As presented in Fig. 2(b), the values of the time constant (τ) depend on both of the driving current and the ambient temperature. It is worth noting that the performance of the time constant (τ) could be divided into two regions. At low aging stresses (Region I), the time constant (τ) decreases sharply but both of injected current and applied temperature are still small and reasonable. In contrast, at high aging stresses (Region II), the time constant (τ) decreases gradually as the temperature increases and the current is large. Therefore, as the accelerated stress up to a certain extent, the increase of the degradation rate in luminous flux could become to keep stability in some value and the phenomena might imply that the real influence of burn-in stresses applied to the treated device should be dynamic variable with the aging.

Figure 3(a) plots the reverse current as a function of aging time for various temperatures and currents on a semi-logarithmic scale. To comply with the commercial specifications, the reverse currents were measured under a reverse bias of −5 V and a constant temperature of 25 °C. As displayed in Fig. 3(a), the different deterioration rates in reverse currents were induced by various accelerating aging stresses and the reverse currents also increased with the aging. In the end of aging experiment, more than two orders of magnitude of reverse current were observed compared to the performance of 1 A/85 °C and 0.35 A/25 °C at −5 V reverse bias. The similar degradation trends appear the strong correlation between luminous fluxes and reverse leakage current. Restated, the increase in reverse leakage current accompanied the optical degradation. The result indicates that the reverse leakage current is one of the indexes to monitor the degradation behavior of LEDs during long-term aging. The further I–V characteristics of the LEDs before and after aging stresses are shown in Fig. 3(b). After the long-term aging stresses, most of I–V curves presented that the diffusion current, generation-recombination current, and the reverse leakage currents increased greatly over except for the stress of 0.35 A/25 °C. InGaN-based LED chips are hetero-epitaxially grown on sapphire substrate and the dislocation density is determined by the crystal growth.[9,10] The reverse leakage currents are mostly associated with the tunneling of carriers through the dislocations and weakly voltage dependent. Therefore, more than 2 orders of magnitude higher leakage current after the aging could be attributed to the higher defect density.[11,12] Consequence, the changes in reverse leakage current could be used to determine whether the increase and distribution of defect density.

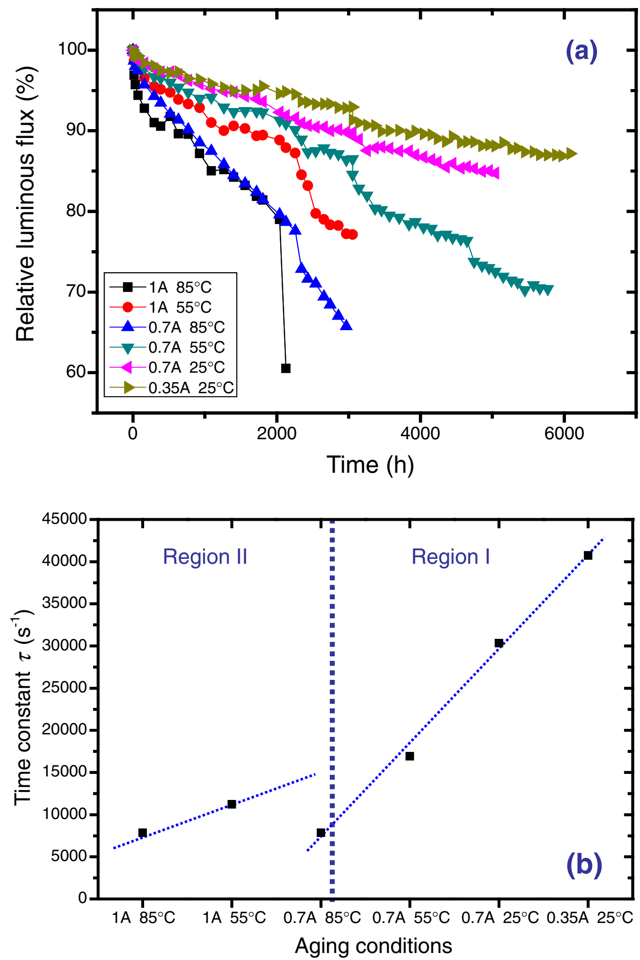

Fig. 2. (Color online) (a) Relative luminous flux as a function of aging time under the different currents and temperatures. (b) Change of the time constant (τ) as a function of the various aging conditions.

The forward I–V curve could be divided into three zones: Zone I for the forward voltage less than 2.3 V, Zone II for the voltage between 2.3 and 2.6 V, and Zone III for the voltage larger than 2.6 V.

© 2011 The Japan Society of Applied Physics

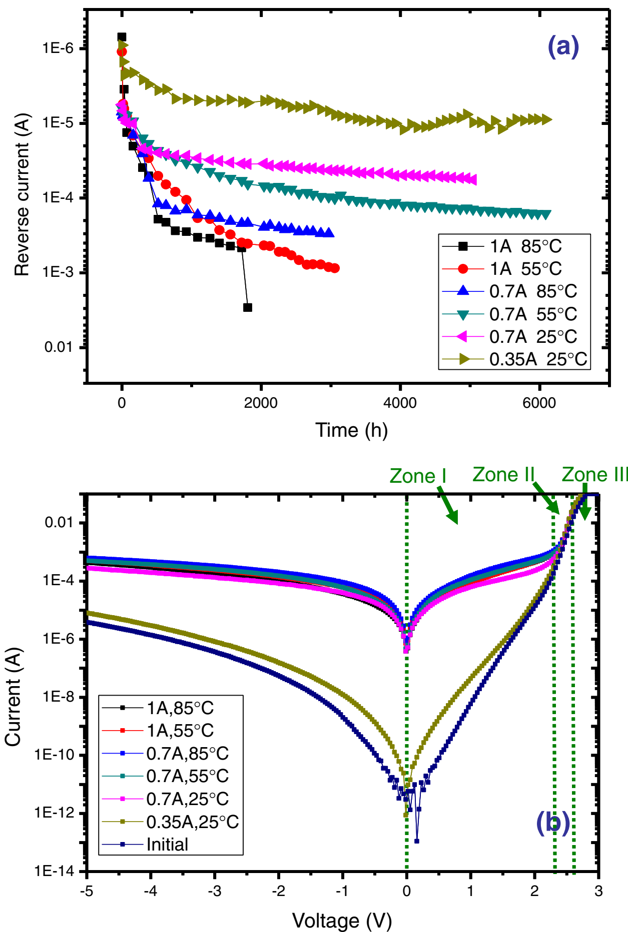

Fig. 3. (Color online) (a) Reverse current as a function of aging time under the various conditions. (b) Semi-log current–voltage (I–V) curve of LED chips measured after six long-term aging tests.

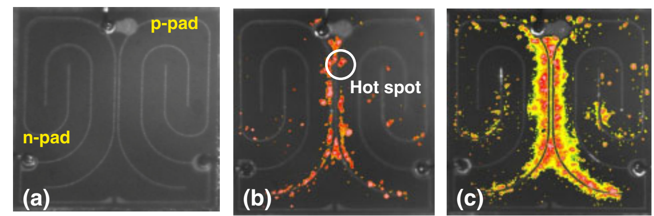

Fig. 4. (Color online) EMMI images of a treated device at 0.7 A/85 °C: (a) before aging, (b) after burn-in 1500 h, and (c) after burn-in 2800 h.

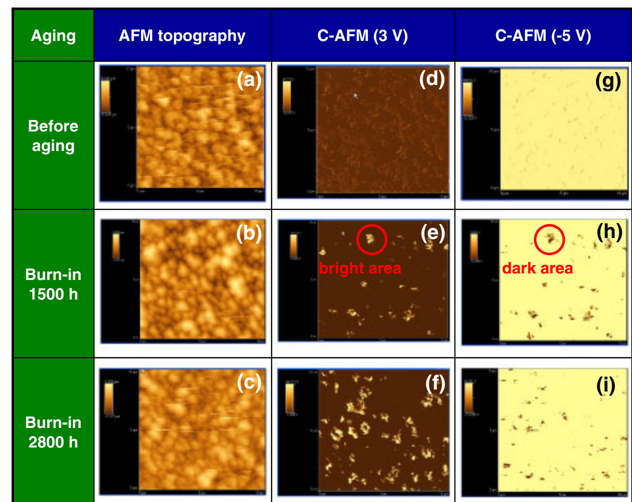

Fig. 5. (Color online) AFM topography and C-AFM current distribution image of a $10 \times 10\,\mu m^2$ area of the treated device at 0.7 A/85 °C. (a–c) AFM topography before aging/burn-in 1500 h/burn-in 2800 h, respectively. (d–f) C-AFM current distribution before aging/burn-in 1500 h/burn-in 2800 h at 3 V. (g–i) C-AFM current distribution before aging/burn-in 1500 h/burn-in 2800 h at −5 V.

Since InGaN-based chip has extremely low intrinsic carrier concentration that in the depletion region is almost zero, the excess current in Zone I is due to carrier recombination in depletion region through trap levels presumably associated with threading dislocations (TDs).[13] Zone II is described in relation to the ideal diode equation for p–n junction assuming the diffusion current. Zone III at high bias voltage, the electrical properties suffer from ohmic loss by the parasitic series resistance (R_s). The increase of R_s is attributed to degradation of the transparent ohmic contact on the top of p-layer and induces the current crowding effect. In additional, the LED degradation is correlated with the variation of doping concentration. During the long-term aging, the change of the effective p-type doping density could be the result of the residue magnesium (Mg) complexes that are reactivated to form Mg–H_2 or Mg–H–N to occur the deep traps. The result would cause the active doping decrease, p-layer resistivity increase, higher forward voltage and series resistance.[14,15]

After the aging, devices exhibit larger leakage current that is more than two orders of magnitudes. Since the reverse leakage current can monitor the degradation transformation of LEDs during long-term aging, the infrared detection tool EMMI is applied to accurately locate the sites and numbers of failures by detecting the excessively abnormal electron-hole pair recombination in a semiconductor device. Figure 4 presents the effect of the increasing aging on the EMMI images of the treated device under the stress of 0.7 A/85 °C. Figures 4(b) and 4(c) indicate the gradually increasing leakage locations and the impact area by hot spots of EMMI images measured at a reverse bias of −5 V. The defect generation in the chips increased the reverse-bias current and strongly related to the threading dislocations of mixed or pure screw character.[16] Furthermore, two p-electrodes arranged through the chip center would cause the serious current crowding and local joule heating to influence LED chip reliability.[17] According to EMMI images, the distribution of hot spots completely matches the electrode geometry and this result also indicates that the lifetime of LED chip closely correlate to the current crowding effect. Consequently, the uniformity of current spreading and thermal distribution would be one of the key indexes to inspect the reliability and endurance of InGaN-based LEDs.

Figure 5 displays the measurements of AFM surface topography and C-AFM current distribution with a typical $10 \times 10\,\mu m^2$ area. As shown in Figs. 5(a)–5(c), the irregular dark areas in surface topography denote V-shape defects with the different diameters that root-mean-square roughness is around 0.43 μm. The current distribution performed in the same region with increasing aging at 3 and −5 V in Figs. 5(d)–5(f) and Figs. 5(g)–5(i), respectively. The bright areas present the forward current distribution and also reflect

© 2011 The Japan Society of Applied Physics

the premature turn-on diodes increasing with aging as shown in Figs. 5(d)–5(f). The premature turn-on could be caused by leakage through surface states at the surroundings of the diodes or defective regions within p–n junction that have a lower barrier height than the main p–n junction. Simultaneously, the dark areas in Figs. 5(g)–5(i) indicate the increasing reverse current with aging and could clearly be associated with the propagation of defective regions. It is worth noticing that both bright areas and dark areas show the similar and symmetrical distribution at 3 and −5 V. Therefore, associated dislocations and V-shape defects in LEDs play a role of leakage paths through p–n junction and are the initial microstructure for the reverse leakage and carrier tunneling observed in the electrical property of devices.[18)]

To further investigate the current crowding effect, we will provide a circuit model of vertical InGaN-based LED and apply C-AFM to observe the microscope electrical property. Firstly, we have investigated the observed leakage current taking both ideal diode characteristics and recombination current into account. Two-dimensional circuit model of InGaN-based LED with the typically vertical structure is shown in Fig. 1. The equivalent electrical circuit could be illustrated by both of resistance and diode without capacitance and inductance because the limitation of LED modulation frequency is around a few MHz range. Accordingly, metals (such as p-electrode and n-electrode) and epilayers (such as substrate, p-GaN and n-GaN) were set as definable series resistances (R_s). The MQWs was represented as an ideal p–n junction diode and parallel resistances (R_p). Therefore, I–V characteristic for InGaN-based LEDs could be represented by[19)]

$$I_{\text{junction}} = I - \frac{V - IR_s}{R_p} = I_s \exp\left[\frac{e(V - IR_s)}{n_{\text{ideal}}kT}\right], \qquad (2)$$

where I_{junction} is the current cross the junction area, I is the total injection current, R_p is the parallel resistance, R_s is the series resistance, I_s is the saturation current, and n_{ideal} is the ideality factor. More meshes with the different electrical diodes employed in the circuit model would naturally lead to a more sophisticated accurate model and analytic result.

Figure 6(a) displays the typical nano-scale regional I–V characteristic of normal area and bright area. The data were measured by locating the conductive nano-tip at a normal area and a bright area as shown in the inset of Fig. 6(a) while the forward bias applied to the n-electrode from 0 to 2.7 V. Under the same forward bias, the premature turn-on characteristic exhibits in the bright area and the mostly common electrical property presents in the normal area. To further explore the local current crowding effect, the C-AFM data were fitting by Shockley equation to meet the higher current operating as the simulated solid lines displayed in Fig. 6(a). According to the above equivalent circuit model in Fig. 1, we assume that single LED chip could be partitioned into 1000 equivalent diodes including the premature turn-on diode (in the bright area) and the common diodes (in the normal area). The ratio of the number of the premature turn-on diode ($N_{\text{premature}}$) and the common diode (N_{common}) were divided into 6 proportions of 1/999, 10/990, 100/900, 500/500, 990/10, and 999/1. Figure 6(b) presents the simulation result that the ratio of current density between the premature turn-on diode ($J_{\text{premature}}$) and the common diode (J_{common})

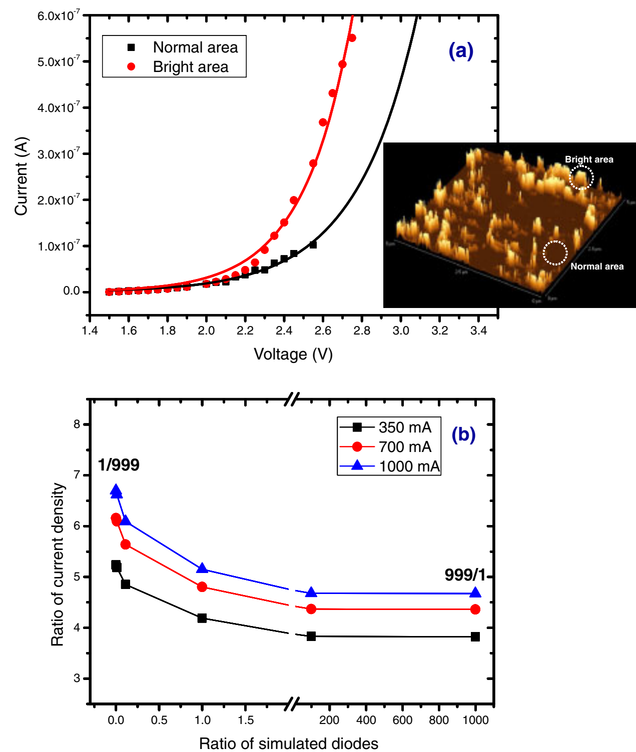

Fig. 6. (Color online) (a) Nano-scale local I–V characteristic of the LED at normal area and bright area. The inset shows three-dimensional current distribution of a treated device at 0.7 A/85 °C after burn-in 2800 h at 3 V. (b) The ratio ($J_{\text{premature}}/J_{\text{common}}$) of current density as a function of the quantity ratio ($N_{\text{premature}}/N_{\text{common}}$) of simulated diodes between premature diodes and common diodes that were divided into 6 proportions from 1/999 (0.001) to 999/1 (999).

drastically decreases with the increasing quantity ratio of simulated diodes ($N_{\text{premature}}/N_{\text{common}}$). The difference of current density in 350, 700, and 1000 mA could almost reach by 5.2, 6.1, and 6.7 times in a single chip as the ratio of the simulated diodes ($N_{\text{premature}}/N_{\text{common}}$) is 1/999. Thus, small electrical mismatch among chip processes could bring very critical current non-uniformity to induce the local degradation or local early failure.

In order to further confirm our explanation as mentioned above and investigate the failure mechanisms, EMMI detection was employed to locate the failure point precisely. Then, FIB was applied to drill a little piece of defect point and TEM was used to investigate the failure interfaces and dislocations as shown in Fig. 7. The left insets in Figs. 7(a) and 7(b) present the EMMI images of a treated chip after the aging and the white circles show the different TEM sampling locations in the same chip. The dislocation densities of hot spot area and an area without any hot spot are 1.94×10^9 cm^{-2} and 3.84×10^9 cm^{-2}, respectively, and the dislocation density of hot spot area is greater than an area without hot spot around two times. The right inset of Fig. 7(b) seems to reveal the phenomenon of threading dislocations through the MQWs in the location of V-shaped defects. For further analyze the variation of threading dislocations, the change in the vicinity of MQWs was observed precisely by more high-resolution TEM. Figures 7(c) and 7(d) show the cross section of MQWs and highlight the dislocation distribution across MQWs. As displayed in Fig. 7(c), stacking faults in the region are evident in the vicinity of MQWs and cause

 © 2011 The Japan Society of Applied Physics

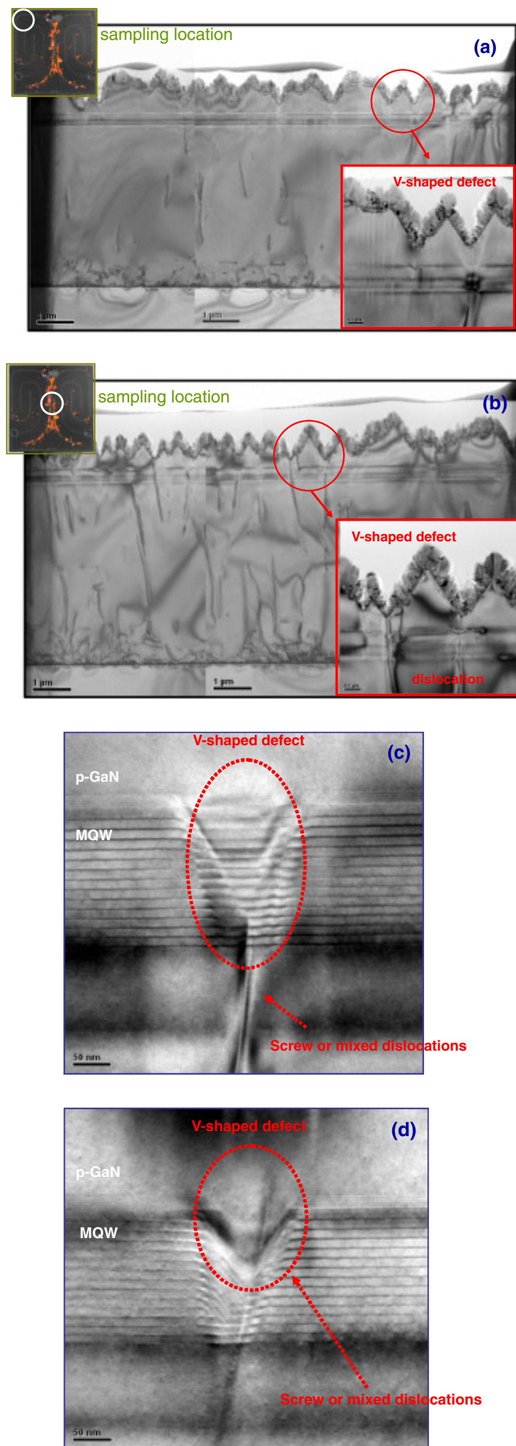

Fig. 7. (Color online) A cross-section images of bright-field TEM of a treated device after the aging of 0.7 A/85 °C. (a) An area without any hot spot at the corner of a chip. (b) Hot spot area in the center of a chip. (c) The region without hot spot around active layers. (d) Hot spot region around active layers.

the distortion in MQWs. It is noting that the threading dislocation did not path through MQWs and no hot spot was captured in this region by EMMI. Figure 7(d) also presents the issue of stacking faults and form V-shaped defect. However, the only difference is that threading dislocation breaks through MQWs to cause short circuits parallel to the diode. The applied current might pass through the short circuits and then the leakage path could be detected by EMMI due to the chip would produce local joule heat instead of light. Consequently, to compare with TEM images between Figs. 7(a) and 7(b), it was obvious that most of the detectable leakage currents could be localized in the periphery of threading dislocations.

Conventional crystalline lattice directions were used for the wurzite structure of GaN and the samples in this experiment were grown on (0001) sapphire substrates. Dislocations in the vicinity of V-shaped defect as displayed in Figs. 7(c) and 7(d) are seen as dark lines propagating in the direction normal to the (0001) substrate. There are three types of threading dislocations display in GaN structures, namely those with Burgers vectors of screw dislocations, mixed dislocations and edge dislocations. The analysis of Burgers vectors implied that edge dislocations were predominantly in the region free of V-shaped defects. The surface V-shaped defects, which possibly initiated prior to the InGaN growth by the growth interruption, were mostly connected with screw or mixed dislocations.[20] Moreover, the threading dislocations of screw and mixed types were also non-radiative recombination center (NRCs) to reduce QW luminescence.[21] and the effect of NRCs would be more apparent as the increase of leakage current in the specific threading dislocations that path through MQWs.

In this study, a complete wafer including over two thousands chips was measured their electrical properties. Sixty specific and representative LED chips were selected to experiment with the aging test and the manufacture process should have high uniformity in a single chip with the size of $1 \times 1\,\mathrm{mm}^2$. Therefore, TEM cross-section images of a treated device after aging demonstrate that the tiny non-uniformity stress would induce the significantly different generation rate of threading dislocations, even within a single chip, which leads to the specific local failure or early degradation. Experimental results as displayed in Figs. 4, 5, and 7 indicate the agreement with the simulations.

4. Conclusions

In the study, we proposed an effective modeling to analyze the issue of non-uniformity current spreading in LED chip and applied the aging test to a commercial 1 W InGaN-based LED chips. The experimental results demonstrate that the increases of reverse leakage current and forward current under the low bias (-2 to 2 V) raised sharply by 10–10^3 times after the aging due to the generation of the local defects. Based on the C-AFM nano-scale regional *I*–*V* performance, the defective area could exhibit premature turn-on characteristics caused by leakage through p–n junction plane that would induce higher current density in the local area. In addition, to compare with the data of EMMI and TEM images, a significant dependence in the distribution of current spreading on the increase of dislocation density was the evidence. It was also found that the evaluation of LED reliability and endurance would strongly correlate to the uniformity of the current spreading. Consequently, for improving the issues of the current crowding and the electrical difference in specific location, a well-designed geometric pattern of electrode and high-stable epitaxial growth process in p-layer could improve LED electrical uniformity and ohmic contact performance to extend the LED lifetime.

© 2011 The Japan Society of Applied Physics

1) E. F. Schubert and J. K. Kim: Science **308** (2005) 1274.
2) M. Asifkhan, M. Shatalov, H. P. Maruska, H. M. Wang, and E. Kuokstis: Jpn. J. Appl. Phys. **44** (2005) 7191.
3) I. Akasaki and H. Amano: Jpn. J. Appl. Phys. **36** (1997) 5393.
4) T. Egawa, T. Jimbo, and M. Umeno: J. Appl. Phys. **82** (1997) 5816.
5) Yu. L. Khait, J. Salzman, and R. Beserman: Appl. Phys. Lett. **53** (1988) 2135.
6) D. L. Barton, M. Osinski, and P. Perlin: Microelectron. Reliab. **39** (1999) 1219.
7) M. Pavesi, M. Manfredi, G. Salviati, N. Armani, F. Rossi, G. Meneghesso, S. Levada, E. Zanoni, S. Du, and I. Eliashevich: Appl. Phys. Lett. **84** (2004) 3403.
8) M. Meneghini, L. Trevisanello, U. Zehnder, T. Zahner, U. Strauss, G. Meneghesso, and E. Zanoni: IEEE Trans. Electron Devices **53** (2006) 2981.
9) X. A. Cao, J. M. Teetsov, M. P. D'Evelyn, D. W. Merfeld, and C. H. Yan: Appl. Phys. Lett. **85** (2004) 7.
10) N. C. Chen, Y. N. Wang, Y. S. Wang, W. C. Lien, and Y. C. Chen: J. Cryst. Growth **311** (2009) 994.
11) S. R. Forrest, M. Didomernico Jr., R. G. Smith, and H. J. Stocker: Appl. Phys. Lett. **36** (1980) 580.
12) J. B. Fedison, T. P. Chow, H. Lu, and I. B. Bhat: Appl. Phys. Lett. **72** (1998) 2841.
13) Z. Z. Bandic, P. M. Bridger, E. C. Piquette, and T. C. McGill: Appl. Phys. Lett. **72** (1998) 3166.
14) P. Kozodoy, S. P. DenBaars, and U. K. Mishra: J. Appl. Phys. **87** (2000) 770.
15) G. Meneghesso, S. Levada, E. Zanoni, G. Salviati, N. Armani, F. Rossi, M. Pavesi, M. Mankedi, A. Cavallini, A. Castaldini, S. Du, and I. Eliashevich: Proc. 42nd Annu. IEEE Reliability Physics Symp., 2004, p. 474.
16) X. A. Cao, J. A. Teetsov, F. Shahedipour-Sandvik, and S. D. Arthur: J. Cryst. Growth **264** (2004) 172.
17) H. Kim, S.-J. Park, H. Hwang, and N.-M. Park: Appl. Phys. Lett. **81** (2002) 1326.
18) P. Perlin, M. Osinsky, P. G. Eliseev, V. A. Smagley, J. Mu, M. Banas, and P. Sartori: Appl. Phys. Lett. **69** (1996) 1680.
19) E. F. Schubert: *Light Emitting Diodes* (Cambridge University Press, Cambridge, U.K., 2006) 2nd ed.
20) F. A. Ponce, D. Cherns, W. T. Young, and J. W. Steeds: Appl. Phys. Lett. **69** (1996) 770.
21) D. Cherns, S. J. Henley, and F. A. Ponce: Appl. Phys. Lett. **78** (2001) 2691.

© 2011 The Japan Society of Applied Physics